More than just recruitment: the X-domain influences catalysis of the first phenolic coupling reaction in A47934 biosynthesis by Cytochrome P450 StaH

Veronika Ulrich[a], Madeleine Peschke[a], Clara Brieke[a] and Max J. Cryle[a,b]

[a.] *Department of Biomolecular Mechanisms, Max Planck Institute for Medical Research, Jahnstrasse 29, 69121 Heidelberg.*

[b.] *EMBL Australia, Monash University, Clayton, Victoria 3800;*

[c.] *The Monash Biomedicine Discovery Institute, Department of Biochemistry and Molecular Biology and ARC Centre of Excellence in Advanced Molecular Imaging, Monash University, Clayton, Victoria 3800.*

Supplementary Information

Table S1. Top ranking structures homologous to StaH identified by Dali search.

PDB code	Chain	Z-score	RMSD Cα [Å]	% Identity	Description (donor organism)	Ref
4TX3	A	54.8	1.2	82	$OxyB_{tei}$-X-domain complex (*Actinoplanes teichomyceticus*)	1
1LG9	A	54.7	1.2	76	$OxyB_{van}$ (*Amycolatopsis orientalis*)	2
1LGF	A	53.3	1.5	76		
1LFK	A	53.2	1.4	76		
4TVF	A	52.5	1.0	82	$OxyB_{tei}$ (*Actinoplanes teichomyceticus*)	3
1UED	A	50.1	1.6	51	$OxyC_{van}$ (*Amycolatopsis orientalis*)	4
2Z36	A	45.4	2.3	34	MoxA (Cyp105, *Nonomuraea recticatena*)	5
3E5L	A	45.4	2.3	37	CYP105P1 (*Streptomyces avermitilis*)	6
4OQS	A	45.3	2.0	41	CYP105AS1 (*Amycolatopsis orientalis*)	7
3ABB	A	44.5	2.0	35	CYP105D6 (*Streptomyces avermitilis*)	8
3TYW	D	44.5	2.4	36	CYP105N1 (*Streptomyces coelicolor*)	*
3O1A	A	44.2	2.4	39	$OxyE_{tei}$ (CYP165D3, *Actinoplanes teichomyceticus*)	9
3OO3	A	44.0	2.1	40		10
4WPZ	A	44.1	2.0	35	CYP107W1 (*Streptomyces avermitilis*)	11
3EJB	B	40.6	2.4	29	$P450_{BioI}$ (CYP107H1, *Bacillus subtilis*)	12
4PXH	E	38.3	3.0	25	PCP_7-$P450_{sky}$ complex (CYP163B3, *Streptomyces sp. ACTA 2897*)	13
4PWV	A	38.0	3.1	25		
4L0F	A	37.6	2.5	25	$P450_{sky}$ (CYP163B3, *Streptomyces sp. ACTA 2897*)	14

*unpublished

Table S2. Loading efficiencies of PCP-X constructs.

	Tei7-L-Hpg$_7$		Tei7-D-Hpg$_7$		Pek7-rac-Hpg$_7$	
	intensity[a]	**normalised (%)**[b]	**intensity**	**normalised (%)**	**intensity**	**normalised (%)**
GB1-PCP-X$_{sta}$	0[c]	0	0	0	n.d.[d]	n.d.
MBP-PCP-X$_{sta}$	1046091	83	940800	75	839205	67
GB1-PCP-X$_{tei}$	933496	74	792822	63	n.d.	n.d.
MBP-PCP-X$_{tei}$	853206	68	602660	48	1256556	100
MBP-PCP$_{sta}$-X$_{tei}$	829242	66	829157	66	942203	75
MBP-PCP$_{tei}$-X$_{sta}$	894886	71	696480	55	643751	51

[a] Intensity = integrated peak areas of substrate peaks observed by HPLC/MS (single ion monitoring).
[b] Intensities normalised using GraphPad Prism 6 with the highest intensity set to 100 %. Values less than 100 % indicate less signal intensity, but not incomplete loading.
[c] Intensity = 0 due to PCP-X precipitation during loading reaction.
[d] n.d. = not determined.

Table S3. List of proteins and primers.

Protein		**Protein ID**	**Gene name**	**Selected sequence range**	**MW [kDa]**	**Primer 5' to 3' (restriction sites underlined)**	
StaH		Q8KLL9	BU52_01285	1-398	47.9	for	CTGCTTAGAATTCATGAGTGGTGACGACCGGCCTCC
						rev	CAGTCTGAAGCTTACCACGTGACCATCAGCCTGC
MBP-PCP-X$_{sta}$		Q8KLL6	-	963-1507	102.8	for	TATCCATGGCGAGCGAAAAGGCGCCGGAG
						rev	ATATCTCGAGCGGACGTTCACGCTCAG
MBP-PCP-X$_{tei}$		Q70AZ6	tcp12	968-1511	103.0	-	
MBP-PCP$_{sta}$-X$_{tei}$	PCP	Q8KLL6	-	963-1041	103.1	for (vector)	GCCGCTCGAGCACCACCACCACCACCACTGAG
						rev (vector)	CTGGGCGTGATTTCGCTGCCAGCGCAC
	X	Q70AZ6	tcp12	1047-1511		for (X)	GCGAAATCACGCCCAGCCCTTGAGGCG
						rev (X)	TGGTGCTCGAGCGGCGCACCGCGTTCC
MBP-PCP$_{tei}$-X$_{sta}$	PCP	Q70AZ6	tcp12	968-1046	102.7	for (PCP)	AGGGCGCCATGGCGTCGGCCAAAGCCC
						rev (PCP)	CTGGGCGCGATTTTGCTGCCAGAGCGC
	X	Q8KLL6	-	1042-1507		for (vector)	CAAAATCGCGCCCAGCCCTTGAAGCTGC
						rev (vector)	GACGCCATGGCGCCCTGAAAATAAAG
X$_{sta}$		Q8KLL6	-	1042-1507	53.2	for	TTTTCAGTGTAGCCATATGGCGCGCCCAGCCCTTGAAG
						rev	GGATGTGACCAAAGCTTCGGACGTTCACGCTCAGCGTCATC

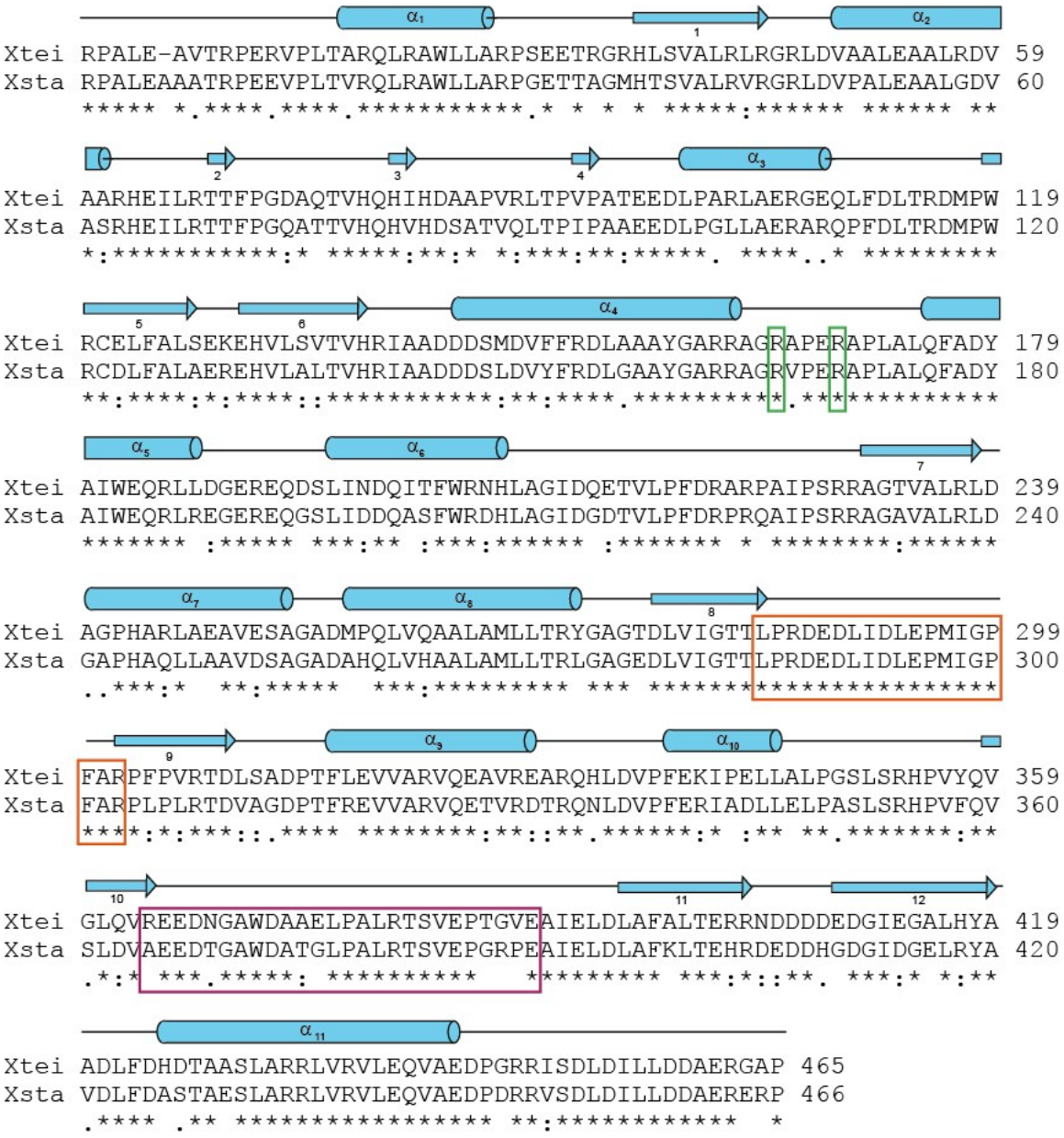

Figure S1. Sequence alignment of X_{sta} and X_{tei}. Secondary structure of the X-domain taken from the crystal structure of the X_{tei}-$OxyB_{tei}$ complex (PDB ID: 4TX3) is shown above the alignment (light blue). The residues crucial for Cytochrome P450 interaction are highlighted (green box) as well as the crossover I (orange box) and crossover II region (magenta box).

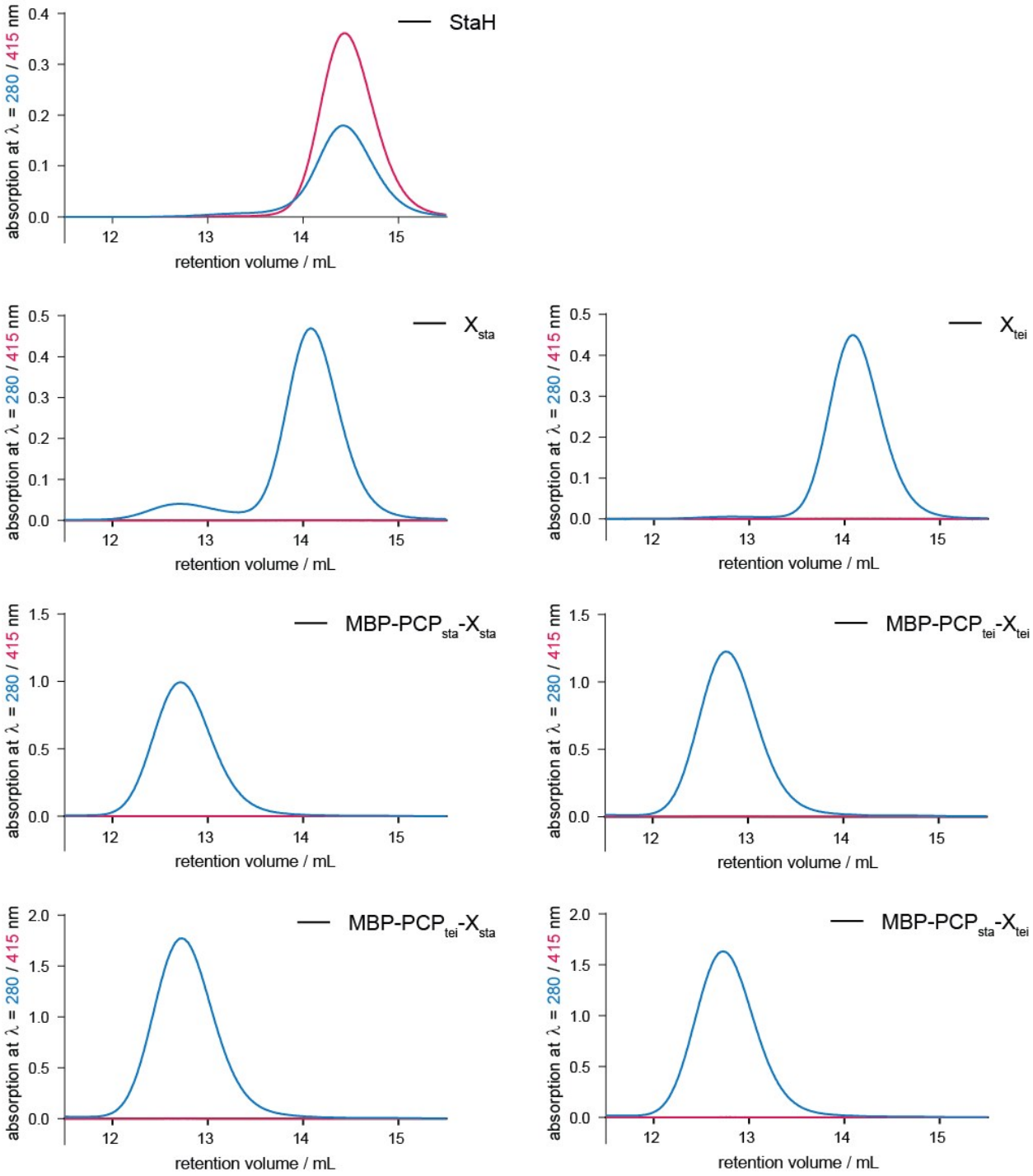

Figure S2. Analysis of StaH as well as A47934 and teicoplanin NRPS constructs using SEC. Individual analysis of these proteins served as controls and were performed in high-salt SEC buffer (50 mM Tris pH 7.4, 300 mM NaCl). Absorptions at both λ = 280 (protein-specific) and 415 (heme-specific) nm were monitored.

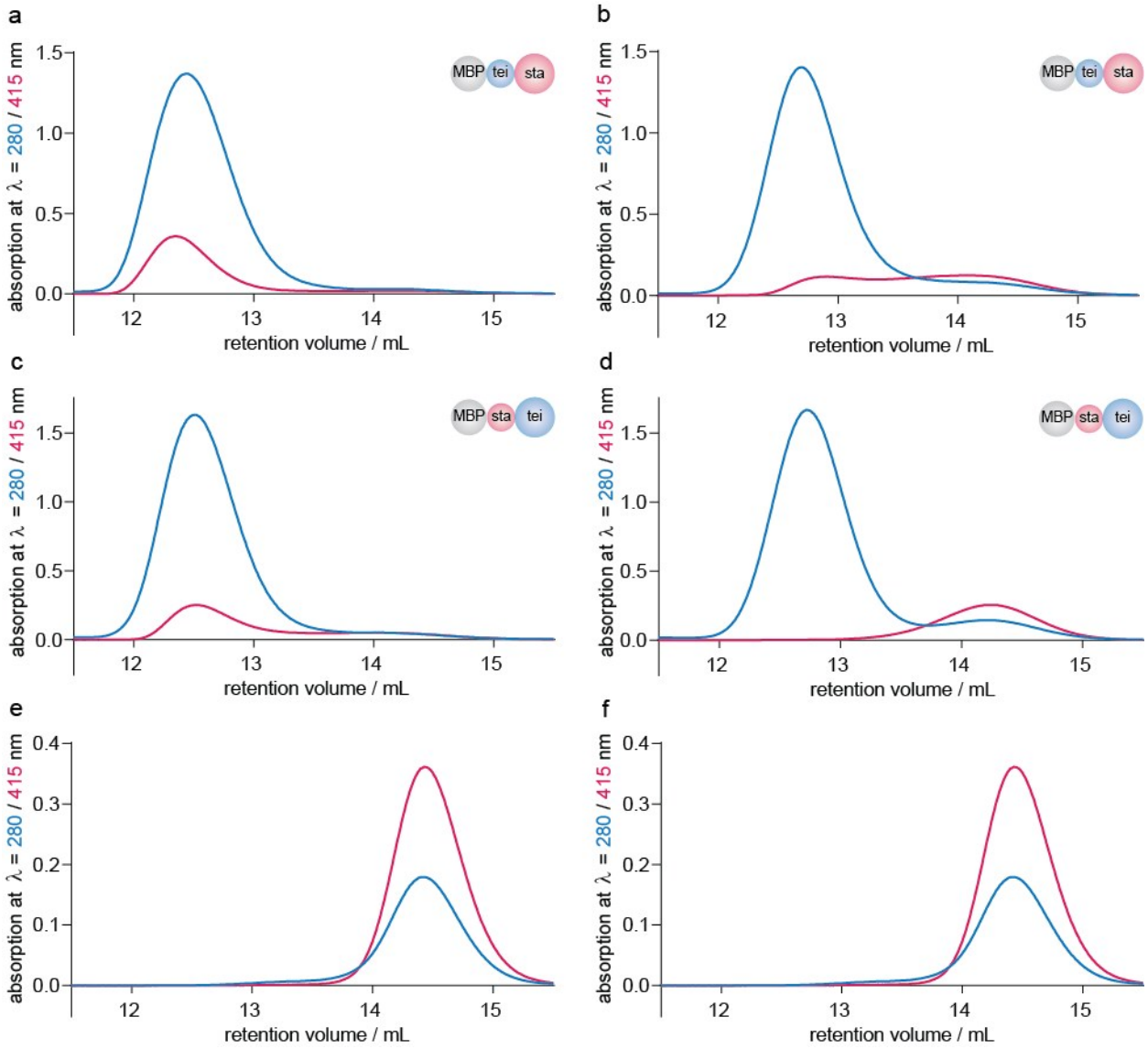

Figure S3. Analysis of StaH interaction with MBP-PCP$_{tei}$-X$_{sta}$ and MBP-PCP$_{sta}$-X$_{tei}$ using SEC. a, c) SEC analysis was performed in standard SEC buffer (50 mM Tris pH 7.4, 150 mM NaCl). b, d, e, f) SEC analysis was were performed in high-salt SEC buffer (50 mM Tris pH 7.4, 300 mM NaCl). Individual StaH (e = f) as well as 1:3 mixtures of StaH to the NRPS constructs (a – d) were analysed. Absorptions at both λ = 280 (protein-specific) and 415 (heme-specific) nm were monitored. Sphere representation of the NRPS constructs is as described in table 2 (main text).

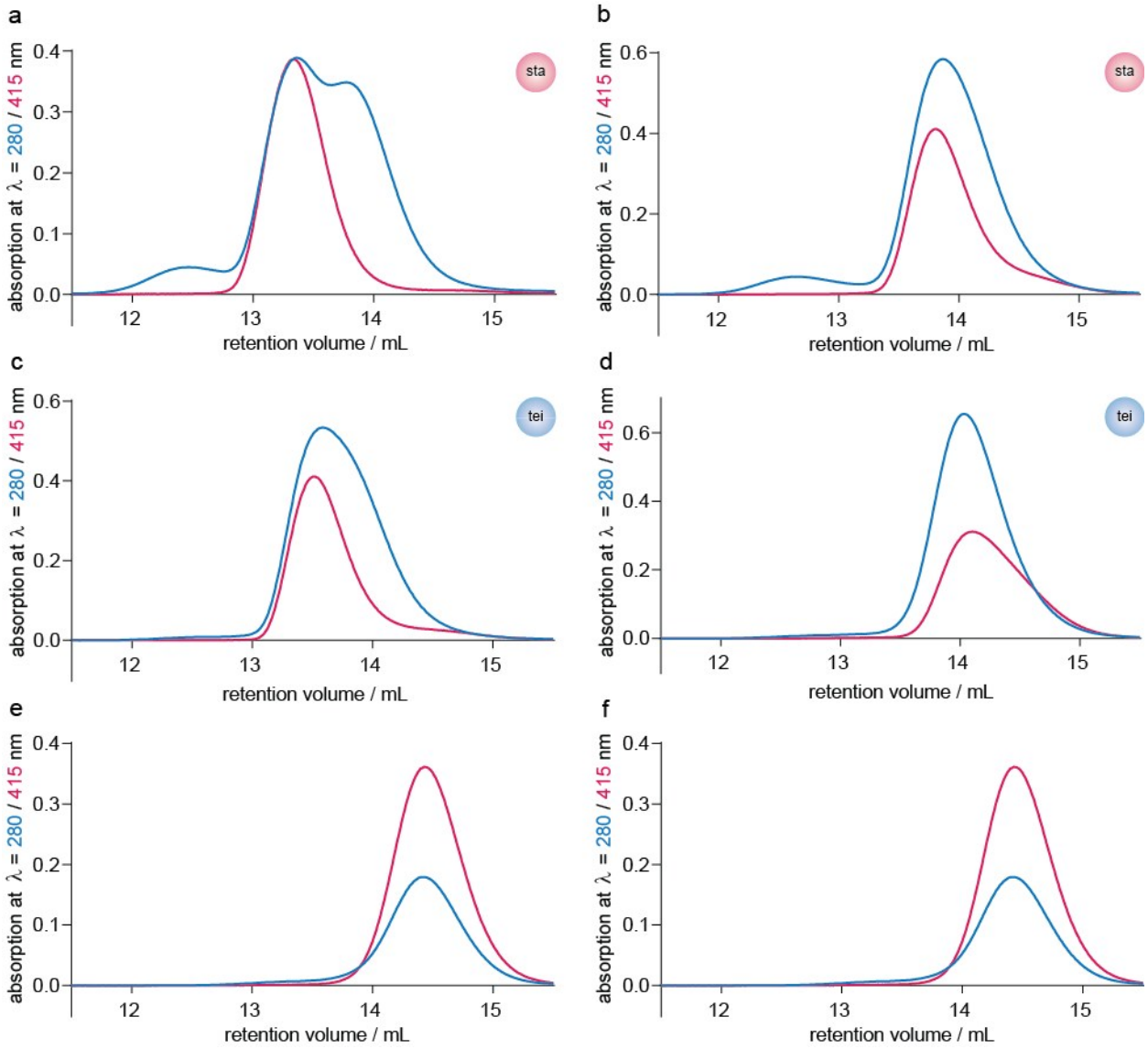

Figure S4. Analysis of StaH interaction with X_{sta} and X_{tei} using SEC. a, c) SEC analysis was performed in standard SEC buffer (50 mM Tris pH 7.4, 150 mM NaCl). b, d, e, f) SEC analysis was performed in high-salt SEC buffer (50 mM Tris pH 7.4, 300 mM NaCl). Individual StaH (e = f) as well as 1:3 mixtures of StaH to the X-domains (a – d) were analysed. Absorptions at both λ = 280 (protein-specific) and 415 (heme-specific) nm were monitored. The spheres represent the individual X-domain with the colour coding described in table 2 (main text).

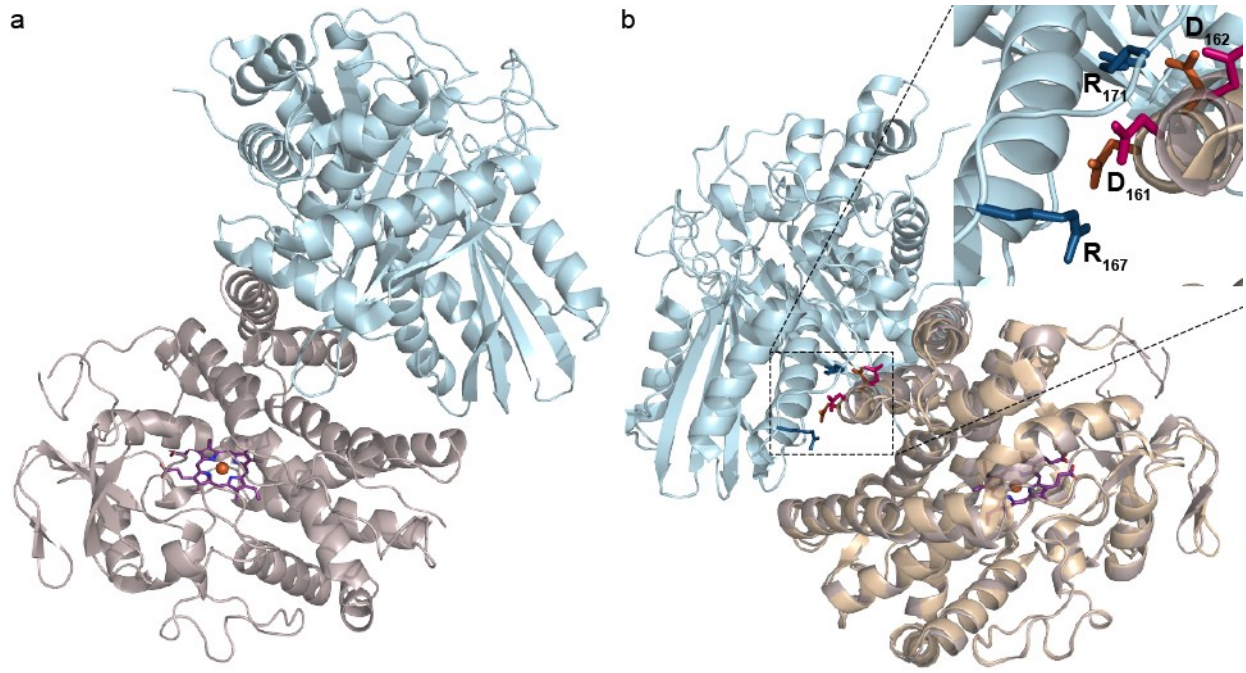

Figure S5. Docking model of X_{tei} (light blue) to StaH (pale red). The heme is shown in purple. a) X_{tei} docks onto the F and G helix of StaH. b) Alignment of $OxyB_{tei}$ (light brown) to StaH with 180° turn in y-axis compared to a). The distance between the interacting residues of X_{tei} (dark blue: R167, R171) and StaH (magenta: D161, D162) is increased compared to the distance between X_{tei} and $OxyB_{tei}$ (orange: D161, D162) from 2.7-3.1 Å to 4.6-7.2 Å.

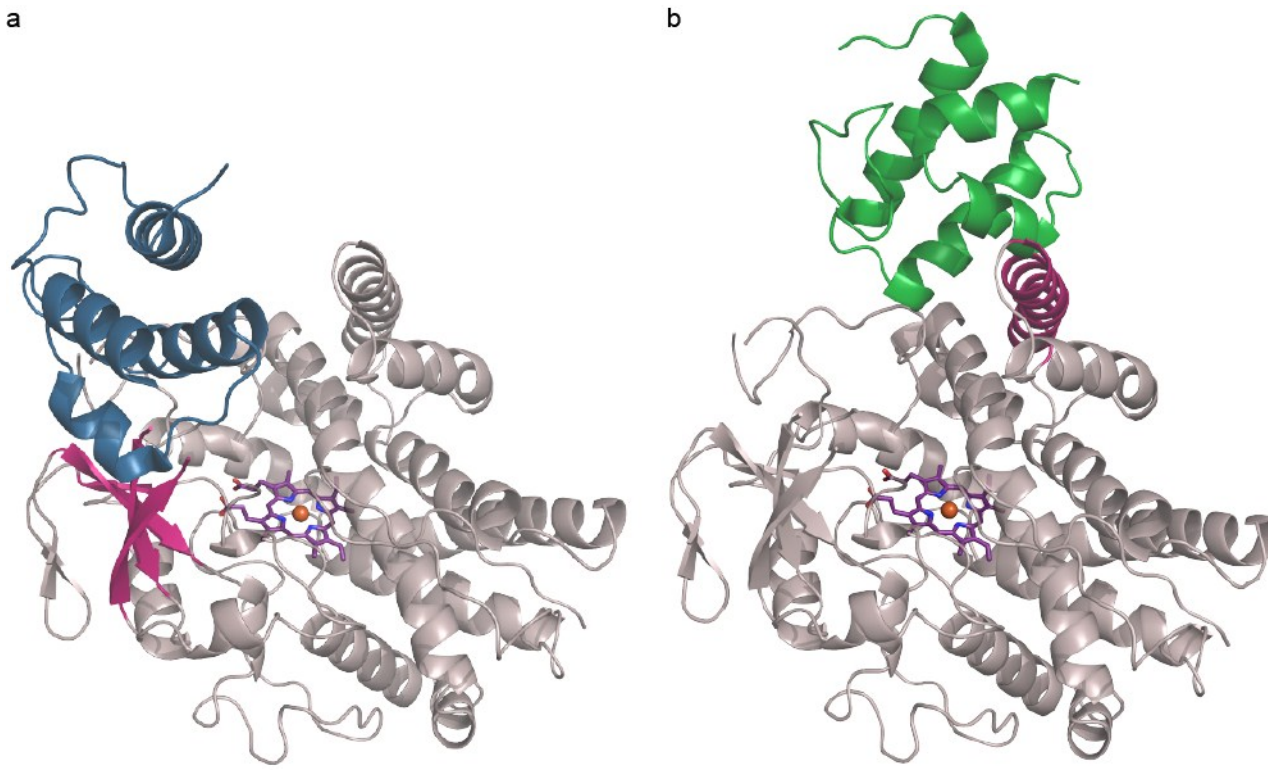

Figure S6. Docking model of ACP from the BioI-ACP complex (PDB ID: 3EJB; a) and PCP from the PCP-$P450_{sky}$ complex (PDB ID: 4PXH; b) to StaH (pale red). The heme is shown in purple. a) ACP (dark blue) docks onto the β-1 region (magenta) of StaH. b) PCP (green) docks onto the G helix (magenta) of StaH.

References

1. K. Haslinger, M. Peschke, C. Brieke, E. Maximowitsch and M. J. Cryle, *Nature*, 2015, **521**, 105-109.
2. K. Zerbe, O. Pylypenko, F. Vitali, W. Zhang, S. Rouset, M. Heck, J. W. Vrijbloed, D. Bischoff, B. Bister, R. D. Süssmuth, S. Pelzer, W. Wohlleben, J. A. Robinson and I. Schlichting, *J. Biol. Chem.* , 2002, **277**, 47476-47485.
3. K. Haslinger, E. Maximowitsch, C. Brieke, A. Koch and M. J. Cryle, *Chembiochem*, 2014, **15**, 2719-2728.
4. O. Pylypenko, F. Vitali, K. Zerbe, J. A. Robinson and I. Schlichting, *J Biol Chem*, 2003, **278**, 46727–46733.
5. Y. Yasutake, N. Imoto, Y. Fujii, T. Fujii, A. Arisawa and T. Tamura, *Biochemical and Biophysical Research Communications*, 2007, **361**, 876-882.
6. L.-H. Xu, S. Fushinobu, H. Ikeda, T. Wakagi and H. Shoun, *Journal of Bacteriology*, 2009, **191**, 1211-1219.
7. K. J. McLean, M. Hans, B. Meijrink, W. B. van Scheppingen, A. Vollebregt, K. L. Tee, J.-M. van der Laan, D. Leys, A. W. Munro and M. A. van den Berg, *Proceedings of the National Academy of Sciences of the United States of America*, 2015, **112**, 2847-2852.
8. L.-H. Xu, S. Fushinobu, S. Takamatsu, T. Wakagi, H. Ikeda and H. Shoun, *The Journal of Biological Chemistry*, 2010, **285**, 16844-16853.
9. M. J. Cryle, J. Staaden and I. Schlichting, *Arch Biochem Biophys*, 2011, **507**, 163-173.
10. Z. Li, S. G. Rupasinghe, M. A. Schuler and S. K. Nair, *Proteins*, 2011, **79**, 1728-1738.
11. S. Han, T.-V. Pham, J.-H. Kim, Y.-R. Lim, H.-G. Park, G.-S. Cha, C.-H. Yun, Y.-J. Chun, L.-W. Kang and D. Kim, *Archives of Biochemistry and Biophysics*, 2015, **575**, 1-7.
12. M. J. Cryle and I. Schlichting, *PNAS*, 2008, **105**, 15696-15701.
13. K. Haslinger, C. Brieke, S. Uhlmann, L. Sieverling, R. D. Sussmuth and M. J. Cryle, *Angewandte Chemie (International ed. in English)*, 2014, **53**, 8518-8522.
14. S. Uhlmann, R. D. Süssmuth and M. J. Cryle, *ACS Chemical Biology*, 2013, **8**, 2586-2596.